

Lattice Boltzmann models for rarefied gases

Victor E. Ambruş^{1,2} and Victor Sofonea¹

¹ Centre for Fundamental and Advanced Technical Research, Romanian Academy
Bd. Mihai Viteazul 24, RO 300223 Timișoara, Romania

² Department of Physics, West University of Timișoara
Bd. Vasile Parvan 4, RO 300223 Timișoara, Romania

ICMMES 2016, Hamburg
19/07/2016



Rarefied gas flows

- The degree of rarefaction can be described using the Knudsen number $Kn = \lambda/L$.
- At large Kn , the continuum approximation is no longer valid, rendering the Navier-Stokes equations inapplicable.
- For mesoscopic systems, the Boltzmann equation can be used to describe the gas dynamics at finite Kn .
- To correctly take into account the mesoscopic nature of the gas, kinetic boundary conditions (diffuse reflection) must be employed on the channel walls.
- At large Kn , the particle-wall interaction becomes dominant in the vicinity of the wall, allowing the distribution function to form a discontinuity with respect to \mathbf{p}_\perp .
- We propose a numerical solution of the Boltzmann-BGK equation based on half-range quadratures.

The Boltzmann distribution function

- In the BGK approximation, the Boltzmann distribution function f obeys:

$$\partial_t f + \frac{1}{m} \mathbf{p} \cdot \nabla f + \mathbf{F} \cdot \nabla_{\mathbf{p}} f = -\frac{1}{\tau} (f - f^{(\text{eq})}),$$

where $\tau \sim \text{Kn}/n$ and $f^{(\text{eq})}$ is the Maxwellian distribution.

- The hydrodynamic variables are given as moments of order N of f :

$$N=0 : \quad \text{number density:} \quad n = \int d^D p f,$$

$$N=1 : \quad \text{velocity:} \quad \mathbf{u} = \frac{1}{nm} \int d^D p f \mathbf{p},$$

$$N=2 : \quad \text{temperature:} \quad T = \frac{2}{Dn} \int d^D p f \frac{\xi^2}{2m}, \quad (\xi = \mathbf{p} - m\mathbf{u}),$$

$$\text{viscous tensor:} \quad \sigma_{\alpha\beta} = \int d^D p \frac{\xi_\alpha \xi_\beta}{m} f - nT \delta_{\alpha\beta},$$

$$N=3 : \quad \text{heat flux:} \quad \mathbf{q} = \int d^D p f \frac{\xi^2}{2m} \frac{\xi}{m}.$$

Diffuse reflection boundary conditions ¹

- The diffuse reflection boundary conditions require:

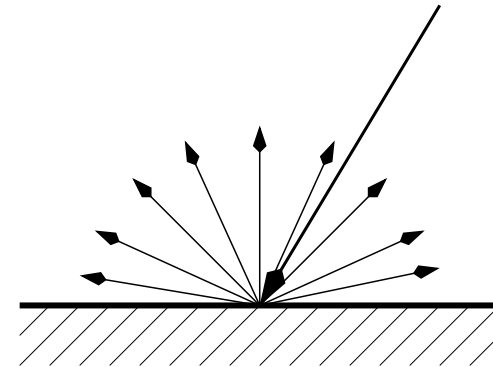
$$f(\mathbf{x}_w, \mathbf{p}, t) = f_w^{(\text{eq})} \equiv f^{(\text{eq})}(n_w, \mathbf{u}_w, T_w) \quad (\mathbf{p} \cdot \chi < 0),$$

where χ is the outwards-directed normal to the boundary.

- n_w is fixed by requiring zero mass-flux through the boundary:

$$\int_{\mathbf{p} \cdot \chi > 0} d^D p f(\mathbf{p} \cdot \chi) + \int_{\mathbf{p} \cdot \chi < 0} d^D p f_w^{(\text{eq})}(\mathbf{p} \cdot \chi) = 0$$

- Diffuse reflection requires the computation of integrals of f and $f^{(\text{eq})}$ over half of the momentum space.



¹S. Ansumali, I.V. Karlin, Phys. Rev. E **66** (2002) 026311.

Discretisation of the momentum space

- The essence of LB is the transition from the continuum momentum space to discrete momenta, while preserving the transport equations up to a given order.
- Through discretisation, $f \rightarrow f_k$ does not necessarily describe the population corresponding to \mathbf{p}_k ; instead, \mathbf{p}_k are chosen such that:

$$\int d^D p f P_s(\mathbf{p}) \simeq \sum_{s=1}^Q f_k P_s(\mathbf{p}_k),$$

where the number of quadrature points Q is chosen such that = occurs for all $s \leq N$.

- One powerful tool that can achieve this is the integration via Gauss quadratures.²

²F. B. Hildebrand, *Introduction to Numerical Analysis*, 2nd ed. (Dover, New York, 1987).

Full-range Gauss-Hermite models^{3,4}

- For N 'th order accuracy, f can be expanded as:

$$f^{(N)} = \frac{1}{\sqrt{2\pi}} e^{-p^2/2} \sum_{\ell=0}^N \frac{1}{\ell!} \mathcal{F}_\ell H_\ell(p), \quad \mathcal{F}_\ell = \int_{-\infty}^{\infty} dp f H_\ell(p).$$

- The Gauss-Hermite procedure allows the moments of f to be written as:

$$\int_{-\infty}^{\infty} dp f(p) P_s(p) = \sum_{k=1}^Q f_k P_s(p_k), \quad f_k = \frac{w_k \sqrt{2\pi}}{e^{-p_k^2/2}} f^{(N)}(p_k),$$

where the Q quadrature points p_k are the roots of H_Q [i.e. $H_Q(p_k) = 0$] and $w_k = Q!/[H_{Q+1}(p_k)]^2$.

- Equality is ensured for all $0 \leq s \leq N$ when $Q > N$.
- The resulting model is denoted **HLB(Q)**.

³V. E. Ambruş, V. Sofonea, J. Comp. Phys. **316** (2016) 1.

⁴V. E. Ambruş, V. Sofonea, J. Comp. Sci. (2016), doi:10.1016/j.jocs.2016.03.016

Half-range Gauss-Hermite models

- For half-range capabilities, f is split at $p = 0$ as:

$$f(p) = \theta(p)f_+ + \theta(-p)f_-,$$

where f_σ ($\sigma = \pm$) are expanded w.r.t. half-range Hermite polynomials $\mathfrak{h}_\ell(p)$:

$$f_\sigma^{(N)} = \frac{e^{-p^2/2}}{\sqrt{2\pi}} \sum_{\ell=0}^N \mathcal{F}_\ell^\sigma \mathfrak{h}_\ell(|p|), \quad \mathcal{F}_\ell^+ = \int_0^\infty dp f \mathfrak{h}_\ell(p), \quad \mathcal{F}_\ell^- = \int_{-\infty}^0 dp f \mathfrak{h}_\ell(-p).$$

- The half-range moments of f can be computed using:

$$\int_0^\infty dp f(p) P_s(p) = \sum_{k=1}^Q f_k P_s(p_k), \quad \int_{-\infty}^0 dp f(p) P_s(p) = \sum_{k=Q+1}^{2Q} f_k P_s(p_k),$$

where $\mathfrak{h}(p_k) = 0$ for all $1 \leq k \leq Q$ and $p_k = -p_{k-Q}$ for all $Q < k \leq 2Q$.

- For N 'th order accuracy, $Q > N$ on each semiaxis \Rightarrow **2Q quadrature points must be employed on the full axis.**
- The resulting model is denoted **HHLB(Q)**.

³V. E. Ambruş, V. Sofonea, J. Comp. Phys. **316** (2016) 1.

⁴V. E. Ambruş, V. Sofonea, J. Comp. Sci. (2016), doi:10.1016/j.jocs.2016.03.016

Couette flow^{5, 6,}

- 2D/3D flow between parallel plates ($x_+ = -x_- = -0.5$) moving along the y axis.

- Homogeneity assumed along y and z :

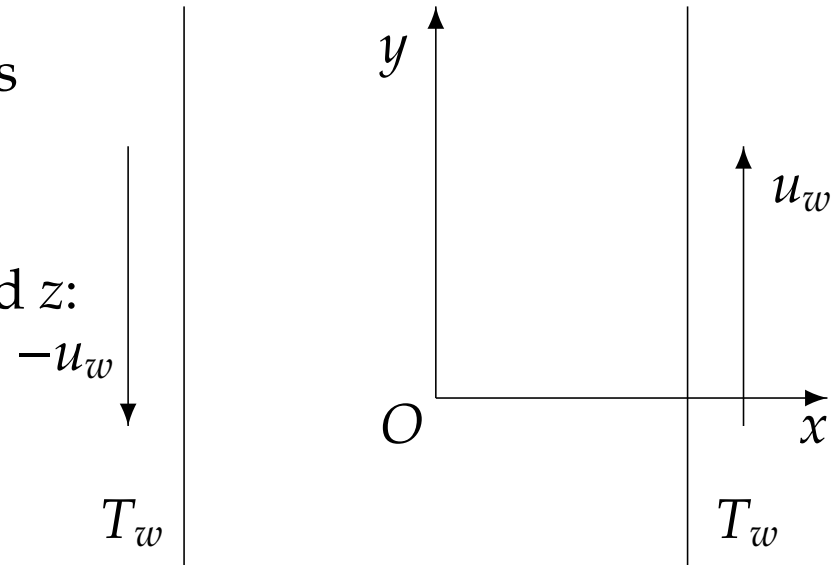
$$\partial_t f + \frac{p_x}{m} \partial_x f = -\frac{1}{\tau} (f - f^{(\text{eq})}).$$

- Diffuse reflection on the x axis.

- $u_w = 0.63$, $T_w = 1.0$.

- Half-range models required to capture the discontinuous character of f induced by the boundary conditions.

- The reference profiles obtained using HHLB(21) \times HLB(4) \times HLB(4).

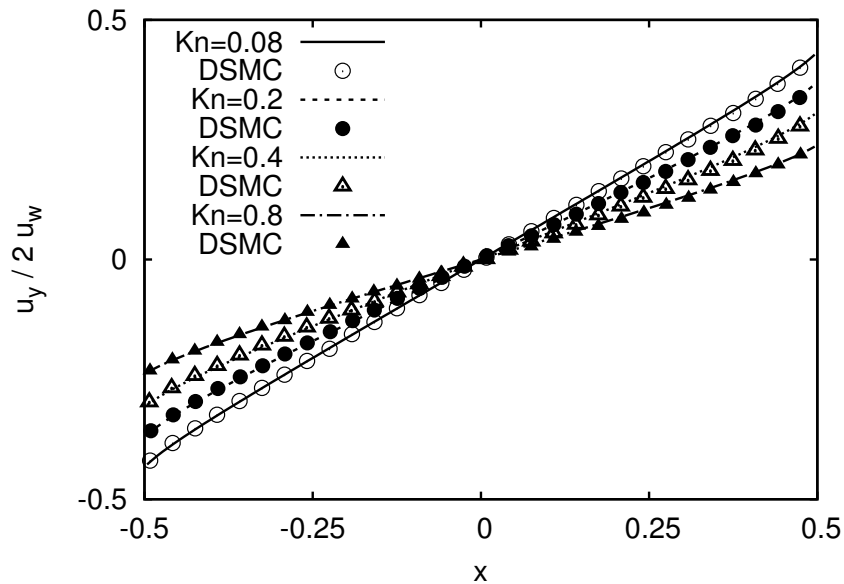


⁵V. E. Ambruş, V. Sofonea, Phys. Rev. E **86** (2012) 016708 [3D, spherical, full-range]

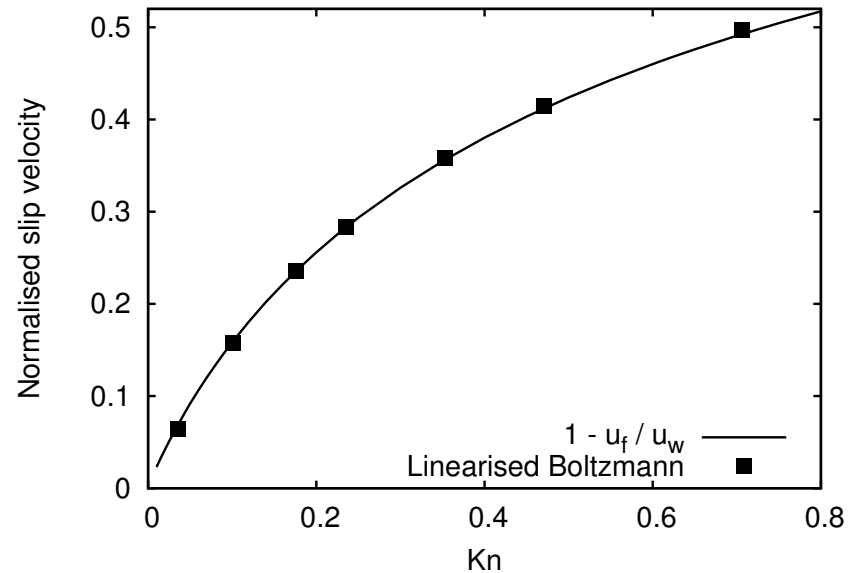
⁶V. E. Ambruş, V. Sofonea, Phys. Rev. E **89** (2014) 041301(R) [3D, Shakhov]

³V. E. Ambruş, V. Sofonea, J. Comp. Phys. **316** (2016) 1 [2D, BGK]

Validation of the reference profiles



(a)



(b)

- DSMC results in (a) and linearised Boltzmann results in (b) obtained from⁷.
- LB results obtained using HHLB(21) on x are in excellent agreement with the DSMC and linearised Boltzmann results.
- The results for the velocity profile are the same for 2D and 3D.

⁷S. H. Kim, H. Pitsch, I. D. Boyd, J. Comput. Phys. **227** (2008) 8655.

³V. E. Ambruş, V. Sofonea, J. Comp. Phys. **316** (2016) 1.

Convergence test

- Purpose: test the dependence of the simulation results on Q_x .
- The following error is calculated for each profile $M \in \{n, u_y, T, q_x, q_y\}$:

$$\varepsilon_M = \frac{\max_x [M(x) - M_{\text{ref}}(x)]}{\Delta M_{\text{ref}}},$$

where $M_{\text{ref}}(x)$ represents the reference profile and ΔM_{ref} is the spread of M_{ref} :[†]

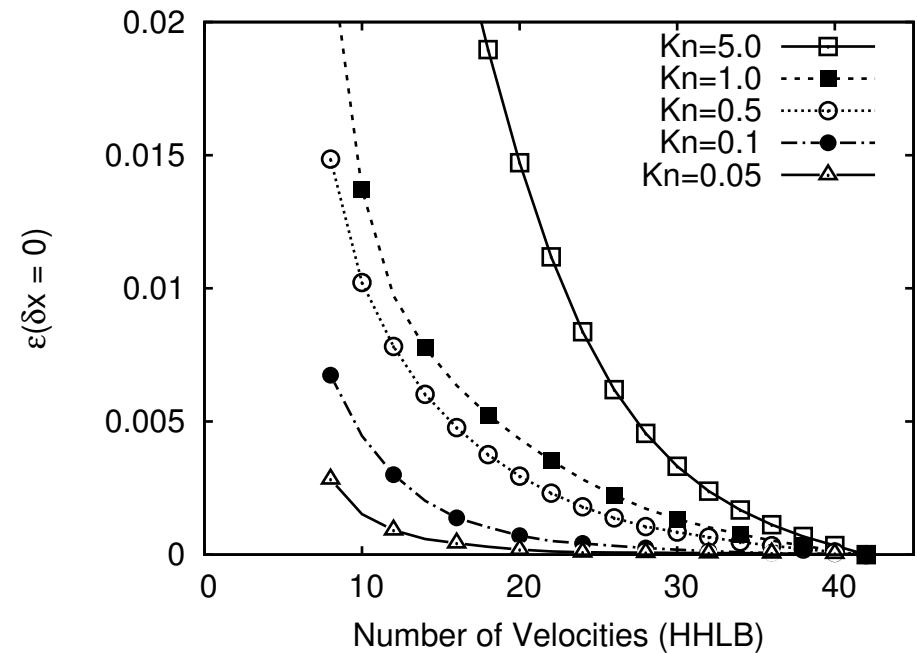
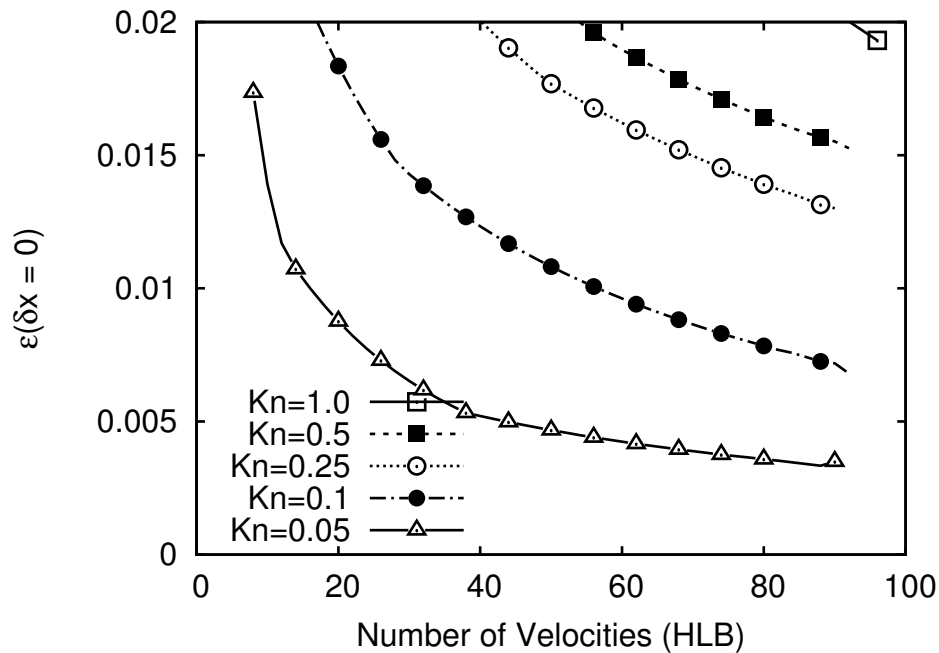
$$\Delta M_{\text{ref}} = \max_x [M_{\text{ref}}(x)] - \min_x [M_{\text{ref}}(x)].$$

- Convergence is achieved when:

$$\varepsilon \equiv \max_M (\varepsilon_M) \leq 0.01.$$

[†]We impose $\Delta M_{\text{ref}} \geq 0.1$ to limit the effects of numerical fluctuations for quasi-constant profiles.

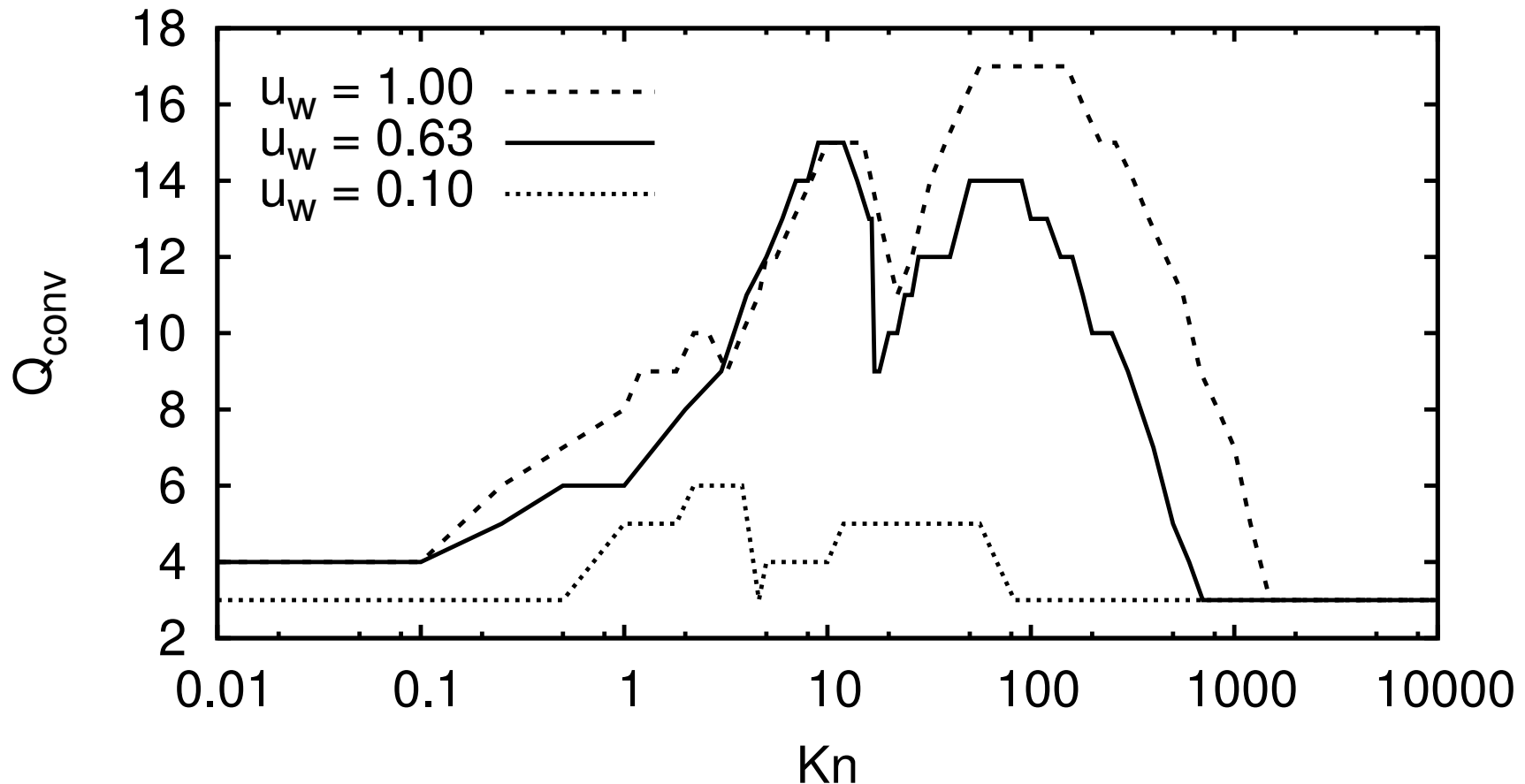
Convergence of HLB vs. HHLB



- 2D Couette-BGK ($u_w = 0.63$).
- The full-range HLB models fail to achieve convergence for Q_x up to 100 for all $Kn \gtrsim 0.25$.
- The half-range HHLB models exhibit fast convergence w.r.t. the increase in Q at all Kn .

³V. E. Ambrus, V. Sofonea, J. Comp. Phys. **316** (2016) 1.

Convergence of HHLB over all Kn

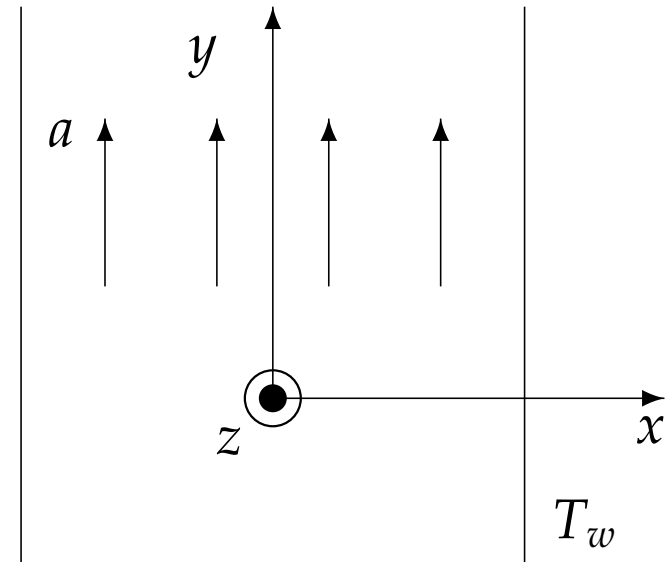


- The HHLB model was used to simulate the Couette flow over the whole $Kn \in [10^{-2}, 100]$.
- Good convergence was observed at all values of Kn .
- For $u_w = 0.1$ (low Mach), *HHLB(6)* employing 12 velocities on the x axis is sufficient to simulate with error $< 1\%$ the entire range of Kn .

³V. E. Ambrus, V. Sofonea, J. Comp. Phys. **316** (2016) 1.

Poiseuille flow⁸,

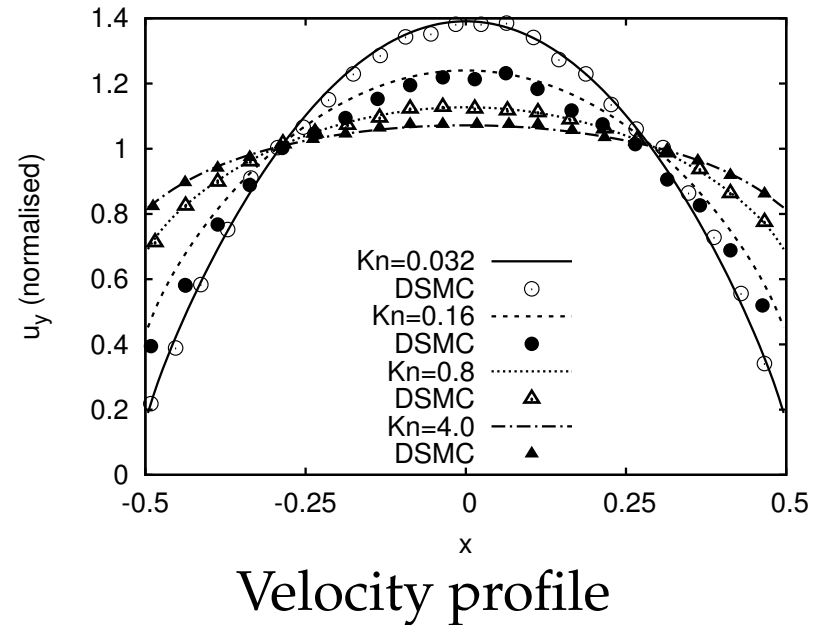
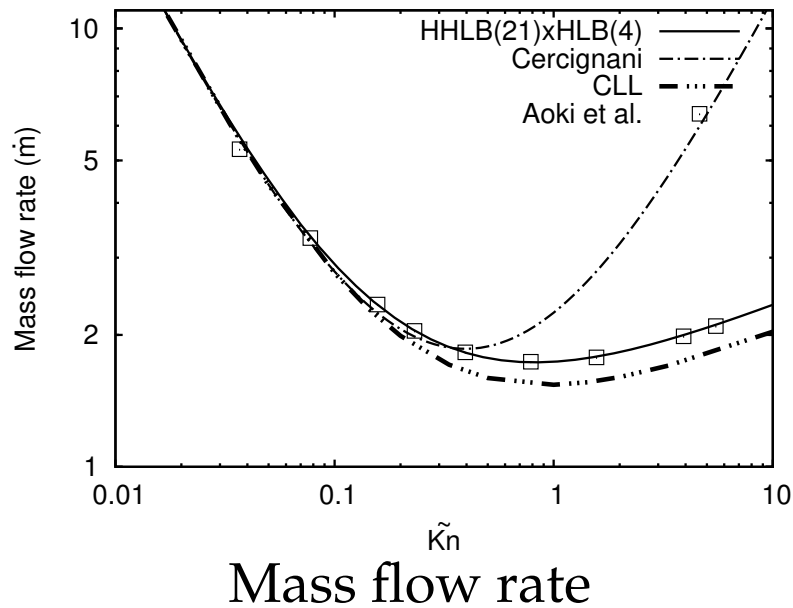
- 2D/3D flow between parallel plates ($x_+ = -x_- = -0.5$) subject to a constant acceleration a along y .
- Diffuse reflection on the x axis.
- $a = 0.1, T_w = 1.0$.
- Half-range models required to capture the discontinuous character of f .
- The reference profiles were obtained using the HHLB(21) model on the x axis.



⁸V. E. Ambruş, V. Sofonea, Interfac. Phenom. Heat Transfer 2 (2014) 235–251 [3D, Shakhov]

⁴V. E. Ambruş, V. Sofonea, J. Comp. Sci. (2016), doi:10.1016/j.jocs.2016.03.016 [2D, BGK]

Validation



- Comparison of mass flow rate against: analytic formula⁹, CLL¹⁰ and Aoki et al.¹¹.
- Comparison of velocity profiles against DSMC results from¹².

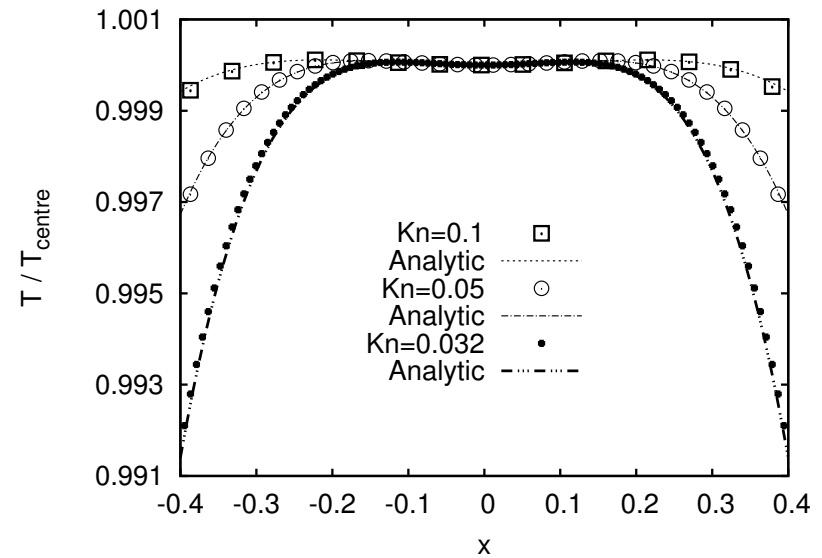
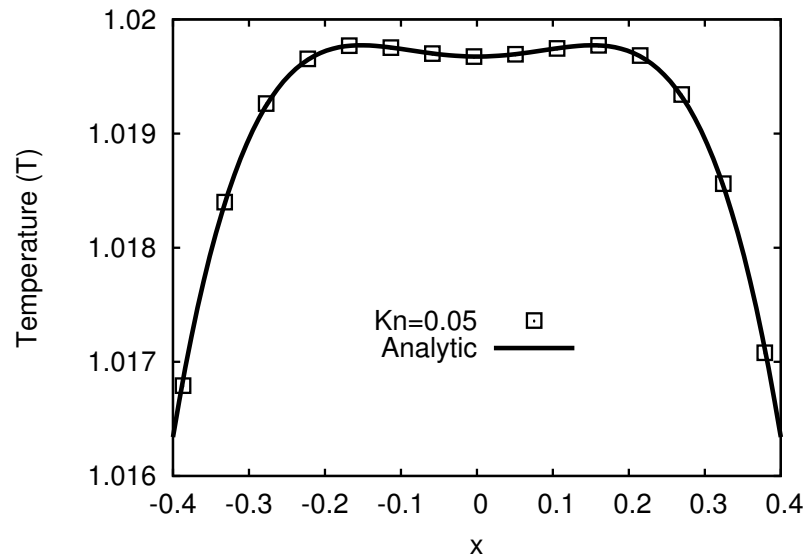
⁹C. Cercignani, *Theory and Application of the Boltzmann Equation* (Scottish Academic Press, Edinburgh, 1975).

¹⁰C. Cercignani, M. Lampis, S. Lorenzani, *Phys. Fluids* **16** (2004) 3426.

¹¹K. Aoki, S. Takata, T. Nakanishi, *Phys. Rev. E* **65** (2002) 026315.

¹²S. H. Kim, H. Pitsch, I. D. Boyd, *J. Comput. Phys.* **227** (2008) 8655.

Temperature dip

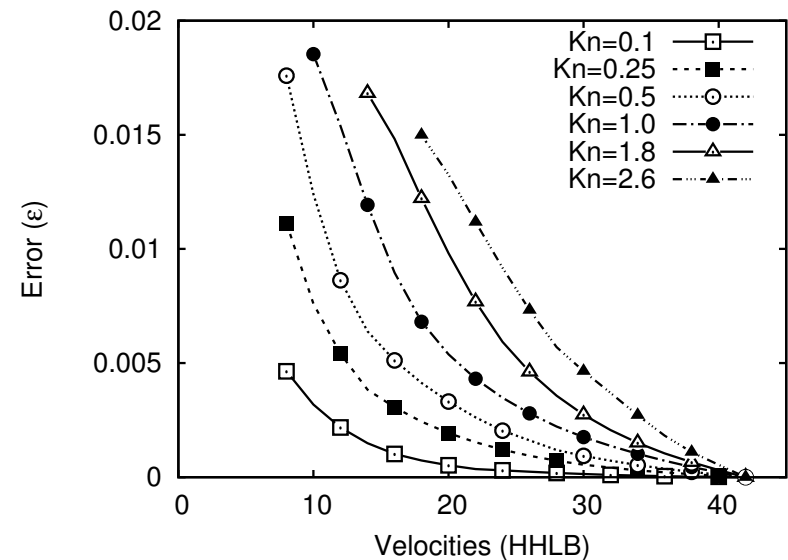
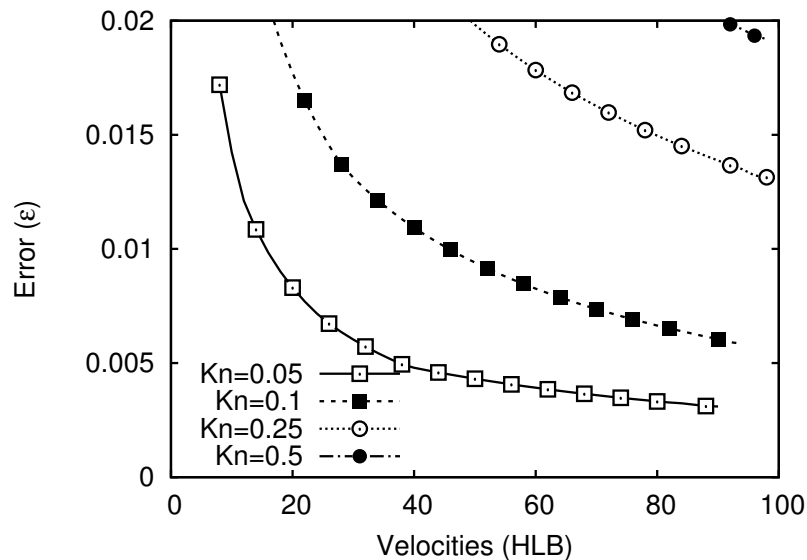


- Comparison with analytic formula¹³ shows excellent agreement:

$$T(x) = T_{\text{centre}} + Ax^2 + Bx^4.$$

¹³S. Hess, M. M. Mansour, Physica A **272** (1999) 481.

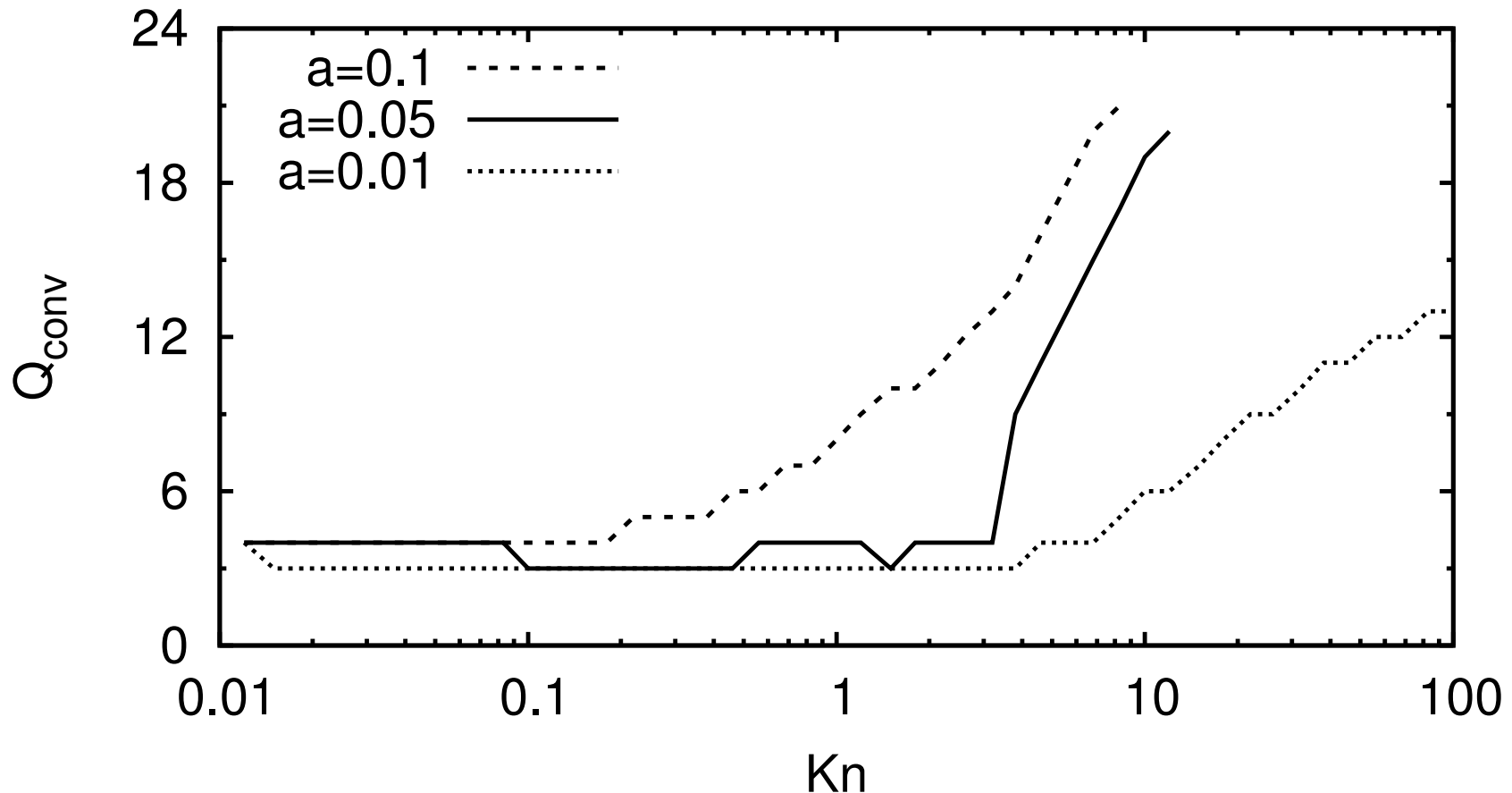
Convergence of HLB vs. HHLB



- The HHLB(Q_x) models exhibit fast convergence.
- The HLB(Q_x) models do not satisfy the 1% test for all $Q_x < 100$ when $Kn \gtrsim 0.25$.

⁴V. E. Ambrus, V. Sofonea, J. Comp. Sci. (2016), doi:10.1016/j.jocs.2016.03.016

Convergence of HHLB over all Kn



- At fixed Kn, Q_{conv} increases with a_y .
- As $\text{Kn} \rightarrow \infty$, convergence can no longer be achieved for all $Q_x < 21$.
- HHLB(3) was sufficient to simulate with error $< 1\%$ for $\text{Kn} \lesssim 3$ for $a_y = 0.01$.

⁴V. E. Ambrus, V. Sofonea, J. Comp. Sci. (2016), doi:10.1016/j.jocs.2016.03.016

Problem with convergence

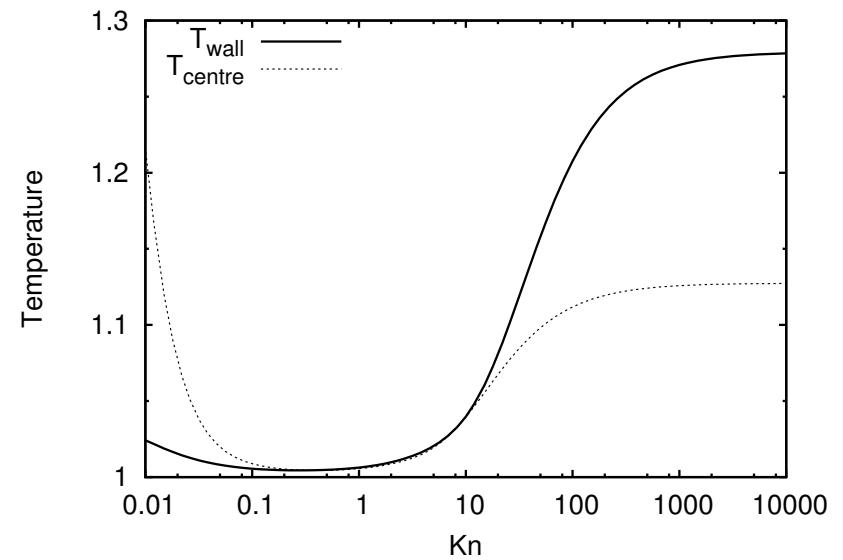
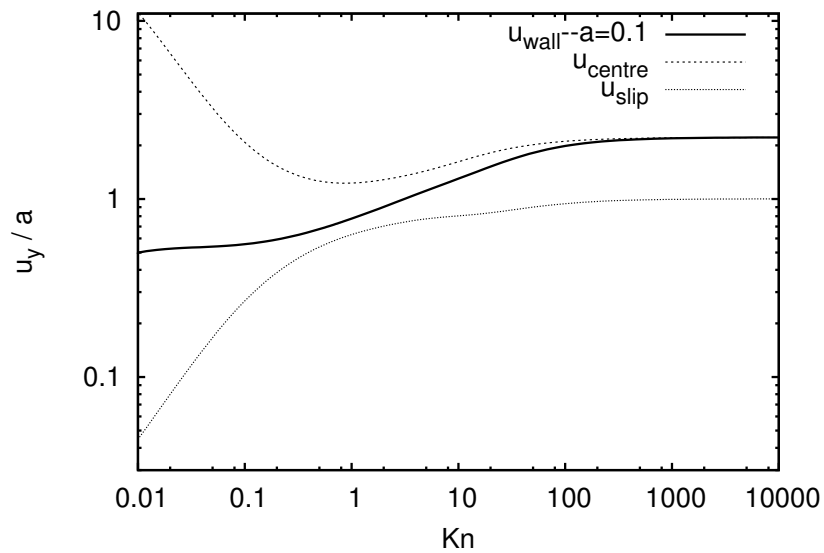
- The solution of the Boltzmann-BGK equation for the 2D Poiseuille flow is:

$$f_{\text{ballistic}} = \frac{n_w}{2\pi m T_w} \exp \left\{ -\frac{1}{2mT_w} \left[p_x^2 + \left(p_y - \frac{m^2 a_y x}{px} - \frac{m^2 a L}{2|p_x|} \right)^2 \right] \right\}.$$

- The analytic solution implies infinite u_y and T in the ballistic regime.
- During the wall interaction, the energy and velocity of particles is reset following the M-B distribution having the wall parameters.
- Infinite velocity/temperature is due to particles with infinite time of flight (i.e. travelling parallel to the walls).
- Such conditions cannot be achieved by HHLB because $p_x = 0$ is not a root of h_Q .
- Thus, the time during which particles are accelerated is that required to travel between the plates, giving rise to a maximum velocity.

⁴V. E. Ambruş, V. Sofonea, J. Comp. Sci. (2016), doi:10.1016/j.jocs.2016.03.016

Velocity and temperature plateau



⁴V. E. Ambruş, V. Sofonea, J. Comp. Sci. (2016), doi:10.1016/j.jocs.2016.03.016

Conclusion

- High order LB models required to simulate thermal flows beyond the Navier-Stokes regime.
- HLB (full-range Hermite LB) requires less velocities at small Kn, but converges very slowly when $\text{Kn} \gtrsim 0.25$.
- Half-space quadratures are necessary in flows between diffuse reflective boundaries at non-negligible Kn.
- Couette flow: HHLB (half-range Hermite) achieves convergence over the full Kn range[†].
- Poiseuille flow: HHLB achieves convergence up to $\text{Kn} \sim 100$ ($\text{Kn} \sim 4$) for $a = 0.01$ ($a = 0.1$).
- This work is supported by a grant from the Romanian National Authority for Scientific Research, CNCS-UEFISCDI, project number PN-II-ID-PCE-2011-3-0516.

Only values of $u_w \leq 1.0$ tested. Convergence is slower as u_w is increased.